Limited Cross-Variant Immunity after Infection with the SARS-CoV-2 Omicron Variant Without Vaccination

Rahul K. Suryawanshi[1†], Irene P Chen[1,2,3,4†], Tongcui Ma[1,16,†], Abdullah M. Syed[1,8,], Noah Brazer[6], Prachi Saldhi[6], Camille R Simoneau[1,3,4], Alison Ciling[1,8], Mir M. Khalid[1], Bharath Sreekumar[1], Pei-Yi Chen[1], G. Renuka Kumar[1], Mauricio Montano[1,17], Miguel A Garcia-Knight[5], Alicia Sotomayor-Gonzalez[6], Venice Servellita[6], Amelia Gliwa[6], Jenny Nguyen[6], Ines Silva[7], Bilal Milbes[7], Noah Kojima[7], Victoria Hess[7], Maria Shacreaw[7], Lauren Lopez[7], Matthew Brobeck[7], Fred Turner[7], Frank W Soveg[1], Ashley F. George[1,14], Xiaohui Fang[15], Mazharul Maishan[15], Michael Matthay[15], Warner C. Greene[1,3,5,17], Raul Andino[5], Lee Spraggon[7], Nadia R. Roan[1,14*], Charles Y. Chiu[3,6,8,16*], Jennifer Doudna[1,8-13*], Melanie Ott[1,3,4*]

[1]Gladstone Institutes, San Francisco, CA, USA.
[2]Biomedical Sciences Graduate Program, University of California San Francisco; San Francisco, CA, USA.
[3]Department of Medicine, University of California San Francisco; San Francisco, CA, USA
[4]Quantitative Biosciences Institute COVID-19 Research Group, University of California San Francisco; San Francisco, CA, USA.
[5]Department of Microbiology and Immunology, University of California, San Francisco, San Francisco, CA, USA
[6]Department of Laboratory Medicine, University of California, San Francisco, San Francisco, CA 94158, USA
[7]Curative Inc., 430 S Cataract Ave San Dimas, CA, USA
[8]Innovative Genomics Institute, University of California, Berkeley, Berkeley, CA, USA
[9]Department of Molecular and Cell Biology, University of California, Berkeley, CA, USA
[10]Molecular Biophysics and Integrated Bioimaging Division, Lawrence Berkeley National Laboratory, Berkeley, CA, USA
[11]Howard Hughes Medical Institute, University of California, Berkeley, Berkeley, CA, USA
[12]Department of Chemistry, University of California, Berkeley, Berkeley, CA, USA
[13]California Institute for Quantitative Biosciences, University of California, Berkeley, Berkeley
[14]Department of Urology, University of California, San Francisco, San Francisco, United States
[15]Department of Medicine and Department of Anesthesia, Cardiovascular Research Institute, University of California San Francisco, San Francisco, CA, USA.
[16]UCSF-Abbott Viral Diagnostics and Discovery Center, San Francisco, CA, USA
[17]Michael Hulton Center for HIV Cure Research at Gladstone; San Francisco, CA, USA

[†]Equal contribution

*Correspondence: melanie.ott@gladstone.ucsf.edu, doudna@berkeley.edu, charles.chiu@ucsf.edu, nadia.roan@gladstone.ucsf.edu

SARS-CoV-2 Delta and Omicron are globally relevant variants of concern (VOCs). While individuals infected with Delta are at risk to develop severe lung disease, Omicron infection often causes milder symptoms, especially in vaccinated individuals[1,2]. The question arises whether the current rampant spread of Omicron could lead to future cross-variant protection, accelerating the end of the pandemic. Here we show that without vaccination, infection with Omicron induces a limited humoral immune response in mice and humans. Sera from mice overexpressing the human ACE2 receptor and infected with Omicron neutralize only Omicron, but no other VOCs, while Delta infection elicits broad cross-variant neutralization. This is not observed with the WA1 ancestral isolate, although exposure to both, WA1 and Delta, but not Omicron, cause high-level viral replication, pro-inflammatory cytokine expression, exhaustion of lung-resident T cells and severe disease in infected animals. Analysis of human sera from unvaccinated, Omicron-infected individuals confirms limited neutralization of other variants besides Omicron itself, while sera from Omicron breakthrough cases show robust cross-variant neutralization in vaccinated individuals. Together, our results indicate that Omicron infection enhances preexisting immunity elicited by vaccines, but on its own may not confer broad protection against Non-Omicron variants in unvaccinated individuals.

Since the beginning of the COVID-19 pandemic, multiple waves of infection have occurred from SARS-CoV-2 VOCs that continue to arise and out-compete preceding variants. VOCs with worldwide relevance are Delta (B.1.617.2) and most recently Omicron (B.1.1.529), while Alpha (B.1.1.7), Beta (B.1.351), and Gamma (P.1) variants spread more locally. Compared to ancestral isolate (WA1 or B.1) Omicron is characterized by a large number of unique mutations in spike as well as in other structural proteins, select nonstructural proteins, and accessory open reading frames**.** Omicron bears over 50 mutations across its genome, including ~37 mutations (28 being unique and 9 overlapping with other variants) in the spike glycoprotein, which may contribute to its antigenic differences[3–9].

The constellation of mutations in the Omicron spike protein has been associated with increased transmission[10], decreased spike cleavage[11], and decreased cell-to-cell fusion[11,12]. Importantly, Omicron spike mutations limit efficacies of neutralizing antibodies generated by previous infections, vaccines, and monoclonal antibody treatment[3–9,13]. Indeed, the risk of breakthrough infections and re-infections is increased with Omicron[13–15]. However, disease severity associated with Omicron is lower than Delta[1,2,13], and prior infection or vaccination reduces the risk of hospitalization with Omicron[16,17]. Pressing questions are how effective Omicron-induced immunity is, and whether it is cross-protective against other variants.

Robust infection of mice and human airway cells by Delta and the ancestral isolate but not Omicron

To answer these questions, we studied WA1, Delta, and Omicron infections in mice. Because WA1 and Delta variants cannot infect regular laboratory mice[18], we used transgenic mice overexpressing human ACE2 (K18-hACE2)[19]. We intranasally infected (10^4 PFU) these mice with the three viral isolates and over seven days monitored their body temperature and weight, which serves as indicators of disease progression (**Fig. 1a**). While Delta- and WA1-infected mice showed progressive hypothermia and severe weight loss during this time, Omicron-infected mice exhibited very mild symptoms with only a small increase in body temperature and no weight loss (**Fig. 1b, c**). Five days after infection, the WA1- and Delta-infected mice were hunched or lethargic, while the Omicron-infected mice appeared completely normal (**Extended Data Fig. 1a**). All of the Omicron-infected mice survived the one-week experiment, while 100% of WA1- and 60% of the Delta-infected animals reached the humane end-point during this time (**Fig. 1d**). This replicates data previously observed in infected individuals, mice, and hamsters that show mild disease with Omicron, but not with Delta and WA1 infections[1,2,20–24].

To assess viral replication dynamics, we quantified infectious particle production (**Fig. 2a, b**), and viral RNA expression (**Extended Data Fig. 2a, b**) in the respiratory tracts and lungs of infected mice over time. Across all time points, high infectious viral titers were present in upper airways (nasal turbinates and bronchi) and lungs of WA1- and Delta-infected mice, whereas Omicron replication was significantly lower in these organs, as previously observed[20–22]. Lung histology showed that Omicron infection resulted in small localized foci of infected cells (marked by nucleocapsid staining, green) (**Extended Data Fig. 1b, c, d).** A similar pattern but enhanced numbers were observed after WA1 infection while Delta infection showed large patches of infected cells, indicative of enhanced cell-to-cell spread, as previously observed with human lung organoids and cell lines[11](**Extended Data Fig. 1b, c, d**). In addition, brain tissue, which is a target for viral replication in K18-hACE2 mice, showed lower Omicron replication four and seven days after infection. Omicron also produced less infectious particles in human airway organoids and in the human alveolar A549 epithelial cell line overexpressing ACE2 relative to WA1 and Delta infections (**Fig. 2c, d**), which is consistent with our findings in the mice.

Inflammatory and T cell markers differ between variants

As severe COVID-19 is associated with cytokine storms in conjunction with exhaustion of T cells[25], we next assessed cytokine expression and T cell phenotypes in infected mouse lungs. While infection with WA1 and Delta readily induced proinflammatory markers of severe COVID, such as CXCL10 and CCL2[26], induction by Omicron was significantly reduced early after infection (**Extended Data Fig. 3a**). Induction of interleukin 1α (IL1α) was not significantly different between the three viral isolates, but trended towards lower expression in Omicron-infected animals two days post-infection (**Extended Data Fig. 3a**). No significant difference between the viral variants were observed in the induction of interferon-α (IFNα) or relevant downstream induced genes such as interferon-stimulated gene 15 (ISG15) and 2'-5'-oligoadenylate synthetase 1 (OAS1) (**Extended Data Fig. 3b**).

To assess whether the pro-inflammatory response we observed in WA1-infected mice is also associated with T cell exhaustion in late infection, we generated single-cell suspensions from the lungs of mock- and WA1-infected mice, and performed Cytometry by Time of Flight (CyTOF) mass spectrometry before and after stimulation with overlapping 15-mer peptides spanning the entire spike protein. tSNE visualization of the CyTOF data corresponding to total immune (CD45+) cells from the unstimulated specimens revealed that both CD4+ and CD8+ T cells of infected mice segregate distinctly from their respective counterparts in the mock-infected mice, indicating profound phenotypic changes in pulmonary T cells upon WA1 infection, including upregulation of activation/exhaustion marker programmed cell death 1 (PD1) on T cells from the infected animals (**Fig. 3a**).

When similar experiments were performed with infection by WA1, Delta, and Omicron, we found elevated expression of not only PD1 but also cytotoxic T-lymphocyte-associated protein 4 (CTLA4, another activation/exhaustion marker) on pulmonary T cells in all infected animals, although to a significantly lesser extent in the Omicron-infected mice (**Fig. 3b, c**). Despite evidence of pulmonary T cell exhaustion in mice infected with all three isolates, functional SARS-CoV-2-specific T cells were still generated in the lungs, as demonstrated by our identification of IFNγ- and TNFα-producing cells specifically in the peptide-stimulated specimens (**Fig. 3d, e, f**), suggesting presence of conserved T cell epitopes in the Omicron variant [27]. These results together suggest that pro-inflammatory cytokines and activated/exhausted pulmonary T cells are elicited by SARS-CoV-2 in a manner that associates with the severity of SARS-CoV-2 infection.

Infection with Delta, but not Omicron, induces cross-variant neutralization

To determine humoral immune responses induced by infection with the three different isolates, we collected sera from mice at seven days after infection, and tested their neutralization efficiency against SARS-CoV-2 isolates: WA1, Alpha, Beta, Delta, and Omicron. We determined the plaque forming units at different serum dilutions and calculated the 50% neutralization titers (NT50) (**Fig. 4**). Sera from uninfected mice showed no neutralization across all variants as expected (**Fig. 4a**) while sera from WA1-infected mice showed effective neutralization of WA1 and Alpha and to a lesser extent Beta and Delta isolates, but no efficacy against Omicron (NT50 6) (**Fig. 4b).** In contrast, Delta infection effectively neutralized all isolates including Omicron (NT50 115), with the least efficacy observed against Beta (NT50 62) (**Fig. 4c**). Omicron infection, however, only induced neutralization of Omicron (NT50 113), but no other isolate (NT50 3–7) (**Fig. 4d**). This was repeated and confirmed in a second experiment where nine days after infection all mice infected with Omicron showed serum neutralization of Omicron (NT50 92), but no other VOC (NT50 7-16) (**Extended Data Fig. 4a**). These results indicate limited cross-variant neutralization induced by Omicron relative to other isolates, which may be due to its highly mutated spike protein or its lower replicative capacity. Notably, Delta and WA1– despite having similar replicative and inflammatory capacities–exhibited different neutralization profiles, underscoring the role of the different spike (and possibly other viral) proteins in eliciting cross-variant neutralization.

These data were confirmed with sera from seven unvaccinated individuals, who had recovered from Omicron infection **(Extended Data Table 1**). These sera showed the same limited cross-variant neutralization as observed in mice with effective neutralization of Omicron itself (NT50 1418), with a ~20-fold decrease in neutralizing titers against non-Omicron isolates (**Fig. 5a**). In contrast, infection with Pre-Omicron SARS-CoV-2 (likely Alpha and Delta isolates, **Extended Data Table 1**) elicited neutralization of all viral isolates (NT50 90–406) except Omicron (NT50 7) (**Fig. 5b**). Sera from uninfected, unvaccinated individuals showed no neutralization across all variants as expected (**Extended Data Fig. 5a).**

Notably, sera from vaccinated individuals with confirmed Omicron breakthrough infection showed a very high level of neutralization against all isolates, including Omicron (NT50 753) (**Fig. 5c**). A similar "boost" in Omicron neutralization was observed after the third shot of the Pfizer/BioNTech vaccine although the NT50 values across all isolates were lower than after Omicron breakthrough infection (**Fig. 5d**). Increasing neutralization of Omicron was also observed at two different time points after breakthrough infection with non-Omicron (likely Delta, based on date of sera collection) (**Extended Data Fig. 5b, c, d)**. This suggests that Omicron infection can effectively boost existing immunity conferred by vaccination against other variants, eliciting "hybrid immunity" that is effective against not only itself but also other variants.

Collectively, our study shows that while the Omicron variant is immunogenic, infection in unvaccinated individuals may not elicit effective cross-neutralizing antibodies against non-Omicron variants. In vaccinated individuals, however, Omicron infection effectively induces immunity against itself and enhances neutralization of other variants. This, together with our finding that Delta infection elicits broad cross-variant neutralization in mice and vaccinated individuals, supports the inclusion of Omicron- and Delta-based immunogens in future heterologous or multivalent vaccination strategies for broad protection against variants.

References

1. Sigal, A. Milder disease with Omicron: is it the virus or the pre-existing immunity? *Nat. Rev. Immunol.* **22**, 69–71 (2022).
2. Wolter, N. *et al.* Early assessment of the clinical severity of the SARS-CoV-2 omicron variant in South Africa: a data linkage study. *Lancet* **399**, 437–446 (2022).
3. Dejnirattisai, W. *et al.* SARS-CoV-2 Omicron-B.1.1.529 leads to widespread escape from neutralizing antibody responses. *Cell* (2022) doi:10.1016/j.cell.2021.12.046.
4. Syed, A. M. *et al.* Omicron mutations enhance infectivity and reduce antibody neutralization of SARS-CoV-2 virus-like particles. *medRxiv* (2022) doi:10.1101/2021.12.20.21268048.
5. Mannar, D. *et al.* SARS-CoV-2 Omicron variant: Antibody evasion and cryo-EM structure of spike protein-ACE2 complex. *Science* eabn7760 (2022).
6. Cao, Y. *et al.* Omicron escapes the majority of existing SARS-CoV-2 neutralizing antibodies. *Nature* (2021) doi:10.1038/s41586-021-04385-3.
7. VanBlargan, L. A. *et al.* An infectious SARS-CoV-2 B.1.1.529 Omicron virus escapes neutralization by therapeutic monoclonal antibodies. *Nat. Med.* (2022) doi:10.1038/s41591-021-01678-y.
8. Hoffmann, M. *et al.* The Omicron variant is highly resistant against antibody-mediated neutralization: Implications for control of the COVID-19 pandemic. *Cell* **185**, 447–456.e11 (2022).
9. Planas, D. *et al.* Considerable escape of SARS-CoV-2 Omicron to antibody neutralization. *Nature* (2021) doi:10.1038/s41586-021-04389-z.
10. Espenhain, L. *et al.* Epidemiological characterisation of the first 785 SARS-CoV-2 Omicron variant cases in Denmark, December 2021. *Euro Surveill.* **26**, (2021).

11. Meng, B. *et al.* SARS-CoV-2 Omicron spike mediated immune escape, infectivity and cell-cell fusion. *bioRxiv* 2021.12.17.473248 (2021) doi:10.1101/2021.12.17.473248.
12. Sato, K. *et al.* Attenuated fusogenicity and pathogenicity of SARS-CoV-2 Omicron variant. *Research Square* (2022) doi:10.21203/rs.3.rs-1207670/v1.
13. Dejnirattisai, W. *et al.* Reduced neutralisation of SARS-CoV-2 omicron B.1.1.529 variant by post-immunisation serum. *Lancet* (2021) doi:10.1016/S0140-6736(21)02844-0.
14. Pulliam, J. R. C. *et al.* Increased risk of SARS-CoV-2 reinfection associated with emergence of the Omicron variant in South Africa. *MedRxiv* (2021).
15. Miyamoto, S. *et al.* Vaccination-infection interval determines cross-neutralization potency to SARS-CoV-2 Omicron after breakthrough infection by other variants. *bioRxiv* (2022) doi:10.1101/2021.12.28.21268481.
16. Report 50 - Hospitalisation risk for Omicron cases in England. *Imperial College London* https://www.imperial.ac.uk/mrc-global-infectious-disease-analysis/covid-19/report-50-severity-omicron/.
17. England, P. H. SARS-CoV-2 variants of concern and variants under investigation in England. *technical briefing 12* (2021).
18. Shuai, H. *et al.* Emerging SARS-CoV-2 variants expand species tropism to murines. *EBioMedicine* **73**, 103643 (2021).
19. Winkler, E. S. *et al.* SARS-CoV-2 infection of human ACE2-transgenic mice causes severe lung inflammation and impaired function. *Nat. Immunol.* **21**, 1327–1335 (2020).
20. Bentley, E. G. *et al.* SARS-CoV-2 Omicron-B.1.1.529 Variant leads to less severe disease than Pango B and Delta variants strains in a mouse model of severe COVID-19. *bioRxiv* 2021.12.26.474085 (2021) doi:10.1101/2021.12.26.474085.

21. Halfmann, P. J. *et al.* SARS-CoV-2 Omicron virus causes attenuated disease in mice and hamsters. *Nature* (2022) doi:10.1038/s41586-022-04441-6.

22. Shuai, H. *et al.* Attenuated replication and pathogenicity of SARS-CoV-2 B.1.1.529 Omicron. *Nature* (2022) doi:10.1038/s41586-022-04442-5.

23. McMahan, K. *et al.* Reduced Pathogenicity of the SARS-CoV-2 Omicron Variant in Hamsters. *bioRxiv* 2022.01.02.474743 (2022) doi:10.1101/2022.01.02.474743.

24. Abdelnabi, R. *et al.* The omicron (B.1.1.529) SARS-CoV-2 variant of concern does not readily infect Syrian hamsters. *Antiviral Res.* **198**, 105253 (2022).

25. Le Bert, N. *et al.* SARS-CoV-2-specific T cell immunity in cases of COVID-19 and SARS, and uninfected controls. *Nature* **584**, 457–462 (2020).

26. Coperchini, F., Chiovato, L., Croce, L., Magri, F. & Rotondi, M. The cytokine storm in COVID-19: An overview of the involvement of the chemokine/chemokine-receptor system. *Cytokine Growth Factor Rev.* **53**, 25–32 (2020).

27. Choi, S. J. *et al.* T cell epitopes in SARS-CoV-2 proteins are substantially conserved in the Omicron variant. *Cell. Mol. Immunol.* (2022) doi:10.1038/s41423-022-00838-5.

28. Sachs, N. *et al.* Long-term expanding human airway organoids for disease modeling. *EMBO J.* **38**, (2019).

29. National Research Council, Division on Earth and Life Studies, Institute for Laboratory Animal Research & Committee for the Update of the Guide for the Care and Use of Laboratory Animals. *Guide for the Care and Use of Laboratory Animals: Eighth Edition*. (National Academies Press, 2011).

30. Neidleman, J. *et al.* mRNA vaccine-induced T cells respond identically to SARS-CoV-2 variants of concern but differ in longevity and homing properties depending on prior

infection status. *Elife* **10**, (2021).

Figure Legends

Fig. 1| Robust infection of K18-hACE2 mice with Delta and ancestral variant, but not Omicron. a, Schematic of the experiment. Fifteen mice per group were intranasally infected with 10^4 PFU of the indicated variant. Body temperature and weight were monitored daily. At the 2, 4, and 7 days post infection (dpi), the upper respiratory tract and lungs were harvested and processed for downstream analysis. n=5 per group **b,** Changes in body temperature of WA1 (grey), Delta (purple), and Omicron (teal) infected mice. Data is shown as the average ± SD and analyzed by 2way ANOVA. ****p<0.0001. **c,** Severe weight loss of WA1- and Delta-infected mice. Data is shown as the average ± SD and analyzed by 2way ANOVA. ****p<0.0001. **d,** Probability of survival of variant infected mice.

Fig. 2| Robust viral replication of WA1 and Delta, but not Omicron, in mice and human airway cells. a, Plaque assay titers from the upper airway (nasal turbinates and bronchus) of WA1- (grey), Delta- (purple), and Omicron- (teal) infected mice at the indicated time points. Data is shown as the average ± SEM at 2 (n=5), 4 (n=5), and 7 (n=2 to 5) dpi analyzed by the student's t-test. *p<0.05, **p< 0.01, ****p<0.0001, n=5, each dot represents infectious virus titer in individual mice. **b,** Plaque assay titers from the lungs of infected mice at the indicated time point. Data is shown as the average ± SEM at each time point and analyzed by the student's t-test, n=5 **p< 0.01, ***p=0.0005. **c,** Plaque assay titers from supernatants of infected human airway organoids (Multiplicity of infection [MOI] of 1). Data is shown as the average ± SEM and analyzed by 2wayANOVA. n=3, *p<0.05. **d,** Plaque assay titers from supernatants of infected A549-ACE2 cells (MOI of 0.1), n=2. Data is shown as the average ± SEM.

Fig. 3. Ancestral and variant of concern SARS-CoV-2 elicit immune responses in lungs of mice| a, T cells from lungs of infected mice (n=3) are phenotypically distinct and express PD1. Single-cell suspensions of lungs from mock infected (top two rows) and WA1-infected (bottom two rows) K18-hACE2 mice were harvested 9 dpi and then analyzed by CyTOF. Shown are tSNE plots gated on total immune cells (CD45+) from the lungs of the mice, colored by expression levels of the antigen listed at the top (red = highest expression, blue = lowest expression). "Islands" of CD4+ and CD8+ T cells unique to the infected mice (identified by the green and purple arrows, respectively, in the third row) express especially high levels of the activation/exhaustion marker PD1, as demonstrated in the right-hand column. **b-c,** T cells from lungs of infected mice (n=3) express elevated levels of the activation/checkpoint antigens PD1 and CTLA4. The proportions of CD4+ and CD8+ T cells expressing PD1, CTLA4, or both PD1 and CTLA4, are indicated. *p<0.05, **p<0.01, ***p<0.001 as assessed using a one-way ANOVA and adjusted for multiple testing using the Bonferroni. **d,** SARS-CoV-2-specific T cells are elicited in lungs of SARS-CoV-2-infected mice. Representative plots corresponding to pulmonary T cells from uninfected (Mock) and WA1-infected K18-hACE2 mice, stimulated for 6 hours with (bottom) or without (top) overlapping SARS-CoV-2 spike peptides. Note SARS-CoV-2-specific T cells (those producing IFNγ and/or TNFα) were only detected in infected mice after peptide stimulation. **e-f,** SARS-CoV-

2-specific T cells are elicited in lungs of mice infected with WA1 (n=6), Delta (n=3), and Omicron (n=3). The proportions of CD4+ and CD8+ T cells expressing IFNg and/or TNFa (gated as shown in *panel C*) are indicated. CD4+ T cell responses trended highest in Delta-infected mice, while CD8+ T cell responses were highest in Delta- and Omicron-infected mice n=3.

Fig. 4| Cross-variant neutralization of SARS-CoV-2 isolates by sera from infected mice. K18-hACE2 mice were infected with $1x10^4$ PFU of WA1, Delta or Omicron. Virus neutralization assay was carried out with sera collected at 7 dpi. Data points in the graph represent individual sera samples showing 50% neutralization titer (NT50) against SARS-CoV-2 isolates. The numbers in parentheses indicate the fold change in neutralization efficacy or resistance of respective isolates relative to NT50 of ancestral isolate (WA1). The grey band at the bottom of the graph indicates the limit of detection. **a-d,** Graphs representing NT50 of sera from a, naïve, **b,** WA1-infected, **c,** Delta-infected, and **d,** Omicron-infected mice against different viral isolates, n=5 in each group. Data are presented as average ± SEM.

Fig. 5| Cross-variant neutralization of SARS-CoV-2 isolates by human sera. a-d, Graphs representing NT50 of variants by sera from **a,** Unvaccinated individuals with confirmed Omicron infection, n=7, **b,** unvaccinated individuals with a pre-Omicron (likely Alpha and Delta) SARS-CoV-2 infection, n=5 **c,** vaccinated individuals with a confirmed Omicron infection against different viral isolates, n=5, and **d,** vaccinated individuals with the pfizer booster n=5. Data points in the graph represent individual sera samples. The grey band at the bottom of the graph indicates the limit of detection. Data are presented as average ± SEM. The details regarding samples (group, age, sex, COVID-19 infection status, vaccination dates and sample collection dates are summarized in Extended data Table 1).

Methods

Cell Culture

Human Lung Organoids

Whole human lung tissue was digested to a single cell suspension and plated in basement membrane extract as previously published[28]. Briefly, organoids were maintained in DMEM supplemented with supplemented with 10% (vol/vol) R-spondin1 conditioned media, 1% B27 (Gibco), 25 ng/mL Noggin (Peprotech), 1.25 mM N-Acetylcysteine (Sigma-Aldrich), 10 mM Nicotinamide (Sigma-Aldrich), 5 nM Herefulin Beta-1 (Peprotech), and 100 µg/mL Primocin (InvivoGen). HAO media is further supplemented with 5 µM Y-27632, 500 nM A83-01, 500 nM SB202190, 25 ng/mL FGF-7, 100 ng/mL FGF-10 (all from Stem Cell Technologies), HAO media was replaced every 3-4 days.

A549 cells expressing ACE2 (A549-ACE2) and Vero cells expressing TMPRSS (Vero-TMPRSS2) were a gift from O. Schwartz and S.P.J. Whelan, respectively. A549-ACE2 and Vero-TMPRSS2 cells were cultured in DMEM supplemented with 10% FBS and blasticidin (20ug/ml) (Sigma) at 37°C and 5% CO_2. Short Terminal Repeat (STR) analysis by the Berkeley Cell Culture Facility on 17 July 2020 authenticates these as A549 cells with 100% probability.

Vero stably co-expressing human ACE2 and TMPRSS2 cells (gifted from A. Creanga and B. Graham at NIH) were maintained at 37°C and 5% CO2 in Dulbecco's Modified Eagle medium (DMEM; Gibco) supplemented with 10% fetal calf serum, 100ug/mL penicillin and streptomycin (Gibco) and 10µg/mL of puromycin (Gibco).

293T cells stably co-expressing ACE2 and TMPRSS2 were generated through sequential transduction of 293T cells with TMPRSS2-encoding (generated using Addgene plasmid #170390, a gift from Nir Hacohen and ACE2-encoding (generated using Addgene plasmid #154981, a gift from Sonja Best) lentiviruses and selection with hygromycin (250 µg/mL) and blasticidin (10 µg/mL) for 10 days, respectively. ACE2 and TMPRSS2 expression was verified by western blot.

SARS-CoV-2 virus culture

SARS-CoV-2/human/USA/USA-WA1/2020 (WA1) (BEI NR-52281), B.1.1.7 (California Department of Health), B.1.351 (BEI NR-54008), B.1.617.2 (BEI NR-55611) and B.1.1.529 (California Department of Health, BA.1)) were used for either animal infection studies, or serum virus neutralization. The virus infection experiments were performed in a Biosafety Level 3 laboratory. Working stocks of SARS-CoV-2 were made in Vero-TMPRSS2 cells and were stored at -80°C until used.

Omicron variant was isolated from a nasopharyngeal swab sample from a patient hospitalized with COVID-19 at UCSF. A 200 uL aliquot of the sample was serially diluted 1:1 with media (DMEM

supplemented with 1x penicillin/streptomycin) in a 96-well plate for 5 dilutions, in duplicate. A 100uL of freshly trypsinized Vero-hACE2-TMPRSS2 cells, resuspended in infection media (made as above but with 2x penicillin/streptomycin, 5ug/mL amphotericin B [Bioworld] and no puromycin) were added to the nasal sample dilutions at 2.5x105 cells/mL concentration. Cells were cultured at 37°C and 5% CO_2 and checked for cytopathic effect (CPE) from day 2-3. Vero-hACE2-TMPRSS2 cells form characteristic syncytia upon infection with SARS-CoV-2, enabling rapid and specific visual evaluation for CPE. Supernatants were harvested on day 3 after inoculation. A 200ul aliquot of P0 was used to infect a confluent T25 flask to generate a P1 culture, harvested after 3 days. Virus stocks were titered by plaque assay and sequence confirmed by nanopore sequencing.

K18-hACE2 mouse infection model

All protocols concerning animal use were approved (AN169239-01C) by the Institutional Animal Care and Use committees at the University of California, San Francisco and Gladstone Institutes and conducted in strict accordance with the National Institutes of Health Guide for the Care and Use of Laboratory Animal[29]. Mice were housed in a temperature- and humidity-controlled pathogen-free facility with 12-hour light/dark cycle and ad libitum access to water and standard laboratory rodent chow.

Briefly, the study involved intranasal infection ($1X10^4$) of 6-8-week-old female K18-hACE2 mice with Delta and Omicron, while WA1 served as a control isolate of SARS-CoV-2. A total of 15 animals were infected for each variant. Five mice from each group were euthanized at day two, four and seven post infection. The brain, upper respiratory tract including bronchus and nasal turbinates and lungs were processed for further analysis of virus replication.

Cellular infection studies

A549-ACE2 cells were seeded into 12-well plates. Cells were rested for at least 24 hours prior to infection. At the time of infection, media containing viral inoculum (MOI 0.01 and 0.1) was added on the cells. One hour after addition of inoculum, the media was replaced with fresh media without viral inoculum. The supernatant was harvested at 24, 48, and 72 hpi for further plaque assays.

Organoid infection studies

Organoids were plated on geltrex-coated plates (ThermoFisher, 12760013) with 100,000 cells per well, and infected at an MOI of 1. Two hours after addition of the inoculum, the supernatant was removed, cells were washed with PBS, and fresh HAO media was added. Supernatant was harvested for a plaque assay at 24 and 48 hours.

Virus neutralization assay

K18-hACE2 mice infected with $1X10^4$ plaque forming units of WA1, B.1.617.2 and B.1.1.529 (n=5). Considering the early humane endpoints with WA1 and B.1.617.2, more animals (n=15)

were infected for these groups. The serum samples from mice were collected at 7 dpi. Mock infected animals served as a control. The serum dilutions (50µL) were made to get final dilution as 1:30, 1:90, 1:270, 1:810, 1:2430, 1:7290 in serum-free DMEM. The dilutions were separately added with 50 PFU (50µL) of SARS-CoV-2 WA1, Alpha, Beta, Delta, and Omicron. The mixture was mixed gently, incubated at 37^0C for 30 mins, followed by a plaque assay. Similar assay was performed for serum samples from omicron infected (5×10^2) mice obtained at 9 dpi and human serum samples acquired from two ongoing clinical trials led by Curative and UCSF or from hospitalized patients at UCSF (**Extended Data Table 1)**. The virus neutralization efficacy of sera were presented as 50% neutralization titer and the average of each variant and compared to others in terms of fold change.

Plaque assays

Tissue homogenates and cell supernatants were analyzed for viral particle formation for *in vivo* and *in vitro* experiments, respectively. Briefly, Vero-TMPRSS2 were seeded and incubated overnight. The cells were inoculated with 10-1 to 10-6 dilutions of the respective homogenates or supernatant in serum-free DMEM. After the 1 hour absorption period, the media in the wells was overlaid with 2.5% Avicel (Dupont, RC-591). After 72 hours, the overlay was removed, the cells were fixed in 10% formalin for one hour, and stained with crystal violet for visualization of plaque forming units.

Quantitative polymerase chain reaction

RNA was extracted from cells, supernatants, or tissue homogenates using RNA-STAT-60 (AMSBIO, CS-110) and the Direct-Zol RNA Miniprep Kit (Zymo Research, R2052). RNA was then reverse-transcribed to cDNA with iScript cDNA Synthesis Kit (Bio-Rad, 1708890). qPCR reaction was performed with cDNA and SYBR Green Master Mix (Thermo Scientific) using the CFX384 Touch Real-Time PCR Detection System (Bio-Rad). See **Extended Data Table 2** for primers sequences. N gene standards were used to generate a standard curve for copy number quantification. N gene standard was generated by PCR using extracted genomic SARS-CoV-2 RNA as template. A single product was confirmed by gel electrophoresis and DNA was quantified by Nanodrop.

CyTOF analysis of mouse lung specimens

The mice used in the CyTOF study were infected with $5x10^2$ PFU of WA1 and monitored for clinical signs of infection (e.g. body weight and body temperature) starting from day 1 to day 9 post infection. CyTOF was conducted similar to methods recently described[30]. Single-cell suspensions of lung tissue specimens processed using the GentleMACS system (Miltenyi) were treated with 25 µM cisplatin (Sigma) for 60 seconds as a viability dye. The cells were then quenched with CyFACS buffer (PBS supplemented with 0.1% BSA and 0.1% sodium azide) and fixed for 10 minutes with 2% paraformaldehyde (PFA; Electron Microscopy Sciences). Cells were then washed twice with CyFACs and frozen at −80°C until CyTOF antibody staining. Prior to

antibody staining, specimens were barcoded using the Cell-ID™ 20-Plex PD Barcoding kit (Fluidigm, South San Francisco, CA, USA). Fc blocking was performed by treating the cells with 1.5% mouse and rat sera (both from Thermo Fisher) for 15 minutes at 4°C. After washing with CyFACS, cells were stained for 45 minutes at 4°C with the cell surface antibodies listed in Extended Table 3. Antibodies were purchased pre-conjugated from Fluidigm, or conjugated using the Maxpar® X8 antibody labeling kit (Fluidigm). After staining, cells were washed with CyFACS and fixed overnight at 4°C in 2% PFA, and then permeabilized for 30 minutes with Foxp3 Fix/Permeabilization Buffer (Fisher Scientific). After two washes with Permeabilization Buffer (Fisher Scientific), cells were Fc blocked again for 15 minutes at 4°C with mouse and rat sera diluted in Permeabilization Buffer. After washing with Permeabilization Buffer, cells were stained for 45 minutes at 4°C with the intracellular antibodies listed in **Extended Data Table 3**. Prior to CyTOF analysis, cells were incubated for 20 minutes with a 1:500 dilution DNA intercalator (Fluidigm), and then washed twice with CyFACS and once with Cell Acquisition Solution (CAS, Fluidigm). Acquisition was performed in the presence of EQ™ Four Element Calibration Beads (Fluidigm) diluted in CAS. Cells were analyzed on a CyTOF 2 instrument (Fluidigm) at the UCSF Parnassus Flow Core. For data analysis, CyTOF datasets were normalized to EQ calibration and manually gated using the FlowJo software (BD Biosciences). tSNE visualizations of the datasets were performed in Cytobank, with default settings.

Histology

Mouse lung tissues were fixed in 4% paraformaldehyde (Sigma 47608) for 24 hours, washed three times with phosphate buffer saline, and stored in 70% ethanol. Briefly, tissues were processed and embedded in paraffin, and tissue sections were stained for SARS-CoV-2 Nucleocapsid (Genetex, GTX135357). The sections were then imaged using Leica Aperio ImageScope.

VLP production

For a 6-well, plasmids CoV2-N (0.67), CoV2-M-IRES-E (0.33), CoV-2-Spike (0.0016) and Luc-T20 (1.0) at indicated mass ratios for a total of 4 µg of DNA were diluted in 200 µL optimem. 12 µg PEI was diluted in 200 µL Opti-MEM and added to plasmid dilution quickly to complex the DNA. Transfection mixture was incubated for 20 minutes at room temperature and then added dropwise to 293T cells in 2 mL of DMEM containing fetal bovine serum and penicillin/streptomycin. Media was changed after 24 hours of transfection and At 48 hours post-transfection, VLP containing supernatant was collected and filtered using a 0.45 µm syringe filter. For other culture sizes, the mass of DNA used was 1 µg for 24-well, 4 µg for 6-well, 20 µg for 10-cm plate and 60 µg for 15-cm plate. Optimem volumes were 100 µL, 400 µL, 1 mL and 3 mL respectively and PEI was always used at 3:1 mass ratio.

VLP luciferase assay

In each well of a clear 96-well plate 50 µL of SC2-VLP containing supernatant was added to 50 µL of cell suspension containing 50,000 receiver cells (293T ACE2/TMPRSS2). Cells were

allowed to attach and take up VLPs overnight. Next day, supernatant was removed and cells were rinsed with 1X PBS and lysed in 20 µL passive lysis buffer (Promega) for 15 minutes at room temperature with gentle rocking. Lysates were transferred to an opaque white 96-well plate and 50 µL of reconstituted luciferase assay buffer was added and mixed with each lysate. Luminescence was measured immediately after mixing using a TECAN plate reader.

Human serum neutralization assay against VLPs

Human serum samples were acquired from two ongoing clinical trials led by Curative and UCSF or from hospitalized patients at UCSF. The Curative clinical trial protocol was approved by Advarra under Pro00054108 for a study designed to investigate immune escape by SARS-CoV-2 variant (University of California, Los Angeles Protocol Record PTL-2021-0007, ClinicalTrials.gov Identifier NCT05171803). Sample specimens were collected from adults (18-50 years) who either had been vaccinated for COVID-19 and/or had a history of COVID-19. Sample acquisition involved standard venipuncture procedure to collect a maximum of 15 ml whole blood, incubation at ambient temperature for 30–60 min to coagulate, centrifugation at 2200–2500 rpm for 15 min at room temperature, and storage on ice until delivered to the laboratory for serum aliquoting and storage at − 80 ºC until use. A quantitative SARS-CoV-2 IgG ELISA was performed on serum specimens (EuroImmun, Anti-SARS-CoV-2 ELISA (IgG), 2606–9621G, New Jersey). Remnant plasma samples from patients hospitalized with COVID-19 at UCSF were obtained from UCSF Clinical Laboratories daily based on availability. Remnant samples were aliquoted and biobanked and retrospective medical chart review for relevant demographic and clinical metadata were performed under a waiver of consent and according to "no subject contact" protocols approved by the UCSF Institutional Review Board (protocol number 10-01116). Plasma samples were also collected through the UMPIRE (UCSF EMPloyee and community member Immune REsponse) study (protocol number 20-33083), a longitudinal COVID-19 research study focused on collection of prospective whole blood and plasma samples from enrolled subjects to evaluating the immune response to vaccination, with and without boosting, and/or vaccine breakthrough infection. The study cohorts included (1) fully vaccinated individuals with either 2 doses of Emergency Use Authorization (EUA) authorized mRNA vaccine (Pfizer or Moderna) or 1 dose of the EUA authorized Johnson and Johnson vaccine. Consented participants came to a UCSF CTSI Clinical Research Service (CRS) Laboratory where their blood was drawn by nurses and phlebotomists. At each visit, two to four 3mL EDTA tubes of whole blood were drawn, and one or two EDTA tubes were processed to plasma from each timepoint. Relevant demographic and clinical metadata from UMPIRE participants were obtained through participant Qualtric surveys performed at enrollment and at each blood draw. Serum samples were heat inactivated at 56°C for 30 mins prior to use in VLP or infection assays. Pre-COVID sera was pooled into one sample.

Acknowledgements

This research is funded by grants from the National Institutes of Health: NIAID R37AI083139 to M.O., NIH/NIAID (F31 AI164671-01) to I.P.C., NHLBI U54HL147127 to M.M. A.M.S is supported by Natural Sciences and Engineering Research Council of Canada (NSERC PDF-533021-2019). M.O. and W.C.G also received support from the Roddenberry Foundation and M.O. received a gift from Pam and Ed Taft. J.A.D. acknowledges support from the National Institutes of Health (R21AI59666) and support from the Howard Hughes Medical Institute and the Gladstone Institutes. N.R. acknowledges support from the Van Auken Private Foundation, David Henke, and Pamela and Edward Taft; and Awards #2164 and #2208 from Fast Grants, a part of Emergent Ventures at the Mercatus Center, George Mason University. C.Y.C thanks the staff at UCSF Clinical Laboratories and the UCSF Clinical Microbiology Laboratories for help in identifying and aliquoting nasal swab and plasma samples. CYC acknowledges support by the Innovative Genomics Institute (IGI) at UC Berkeley and UC San Francisco, US Centers for Disease Control and Prevention contract 75D30121C10991, Abbott Laboratories, and the Sandler Program for Breakthrough Biomedical Research at UCSF. We thank Stanley Tamaki and Claudia Bispo for CyTOF assistance at the Parnassus Flow Core, and the lab of Eliver Ghosn for guidance on lung cell processing. We thank the Gladstone Histology Core. The group also acknowledges support from the James B. Pendleton Charitable Trust. The funders had no role in study design, data collection and analysis, decision to publish, or preparation of the manuscript.

Data availability statement

The datasets generated during and/or analysed during the current study are available in the manuscript or in the Extended data set.

Author Contributions

Conceptualization: RKS, IPC, MO
Investigation: RKS, IPC, TM, AMS, CRS, AC, MMK, BS, PC, AG
Anti sera: NB, PS, AS, VS, AG, JN, IS, BM, NK, VH, MS, LL, MB, FT, FWS, CYC, LS
Omicron virus culture: MAG, MKM, DW, CH, RA
Lung tissue for organoids: XF, MM, MM
BSL3 facility maintenance: MM
Supervision: LS, JAD, NR, CYC, MO
Writing - original draft: RKS, IPC, MO
Writing - reviewing, & editing: RKS, IPC, GRK, WCG, TM, NR, MO

Competing Interests

A.M.S. and J.A.D. are inventors on a patent application filed by the Gladstone Institutes and the University of California that covers the method and composition of SARS-CoV-2 VLP preparations for RNA transduction and expression in cells. J.A.D. is a cofounder of Caribou Biosciences, Editas Medicine, Scribe Therapeutics, Intellia Therapeutics, and Mammoth Biosciences. J.A.D. is a scientific advisory board member of Vertex, Caribou Biosciences, Intellia Therapeutics, eFFECTOR Therapeutics, Scribe Therapeutics, Mammoth Biosciences, Synthego, Algen Biotechnologies, Felix Biosciences, The Column Group, and Inari. J.A.D. is a director at Johnson & Johnson and Tempus and has research projects sponsored by Biogen, Pfizer, AppleTree Partners, and Roche. C.Y.C. is the director of the UCSF-Abbott Viral Diagnostics and Discovery Study and receives research support from Abbott Laboratories. C.Y.C. also receives support for SARS-CoV-2 research unrelated to this study from Mammoth Biosciences.

Fig. 1

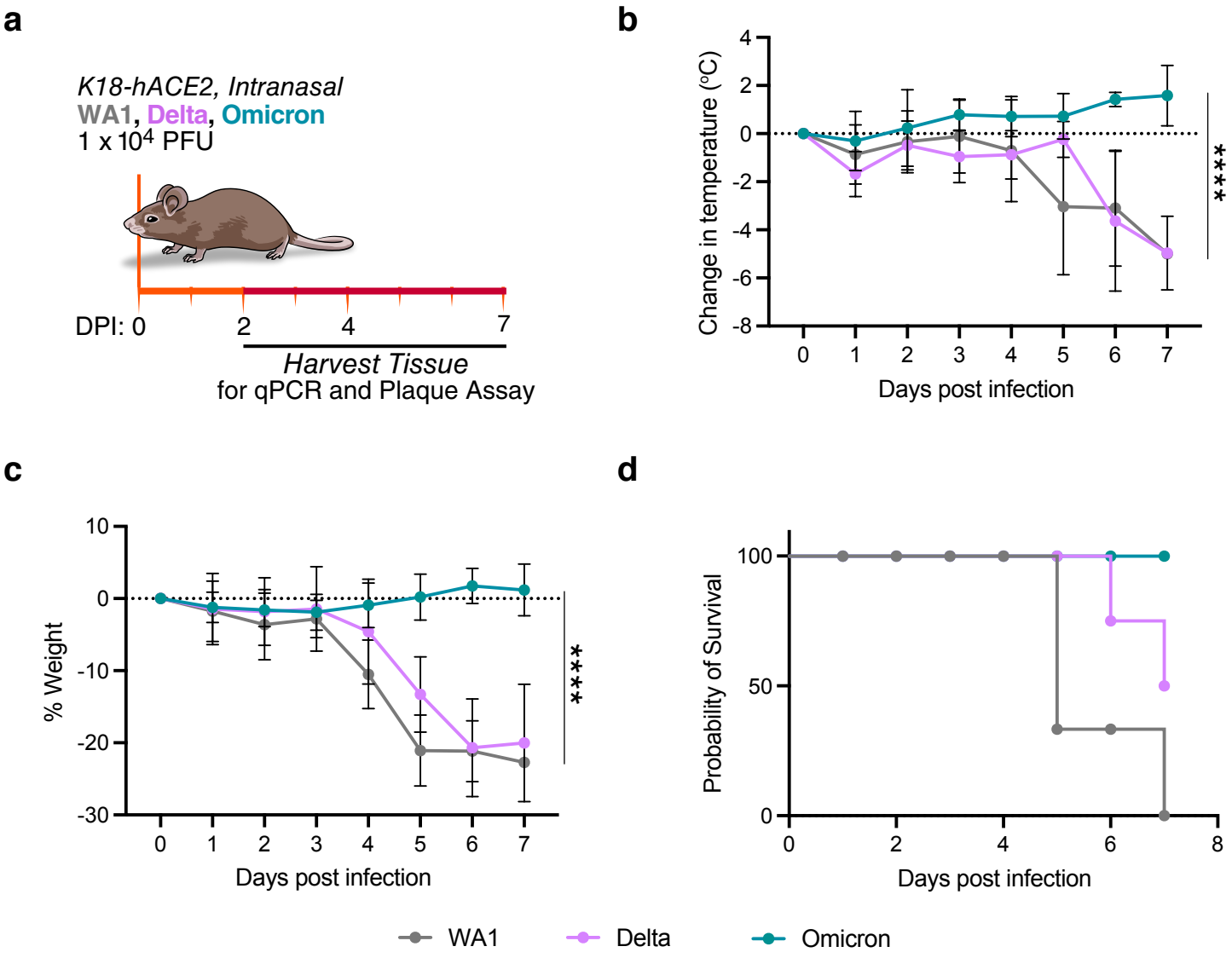

Fig. 2

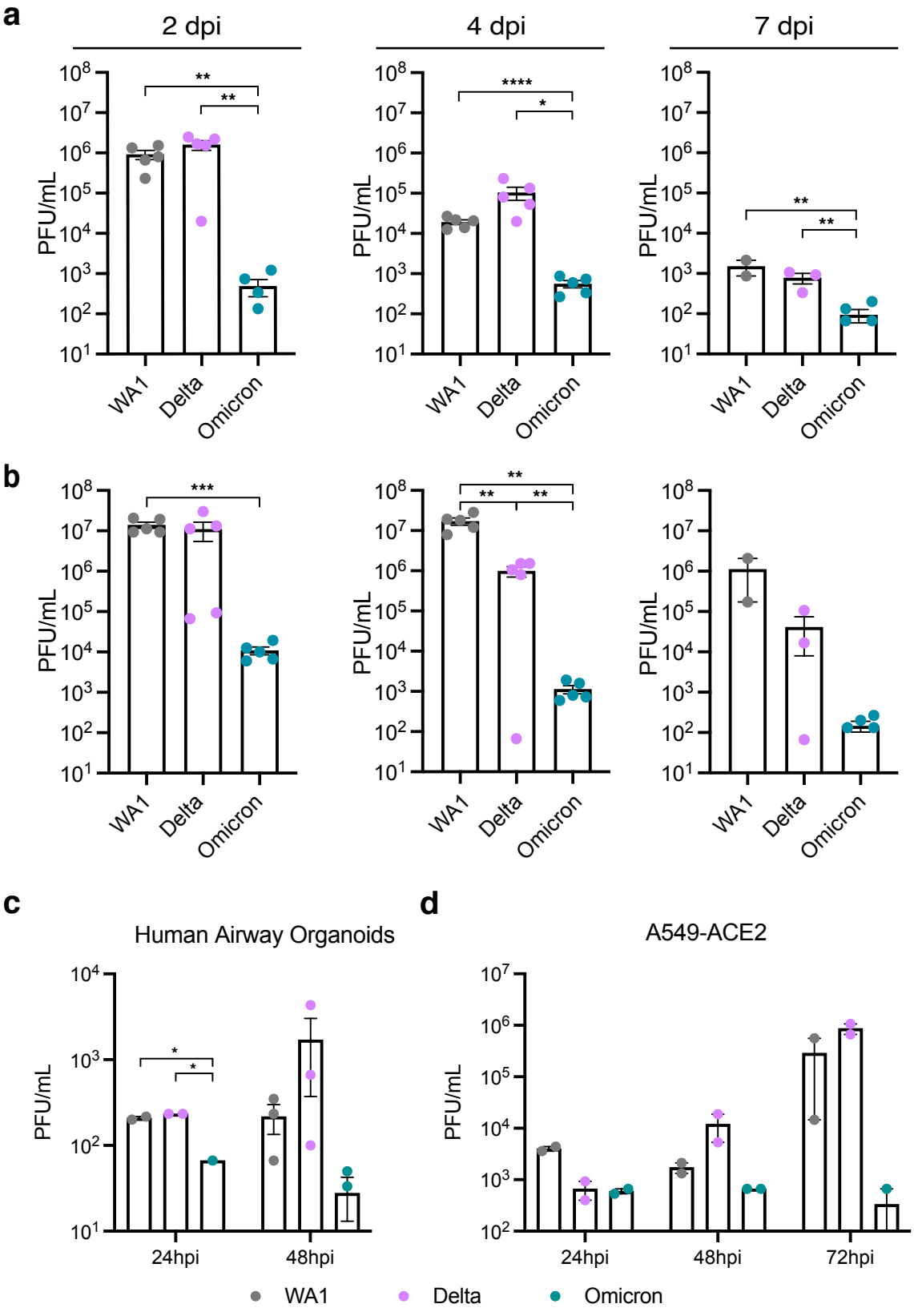

Fig. 3

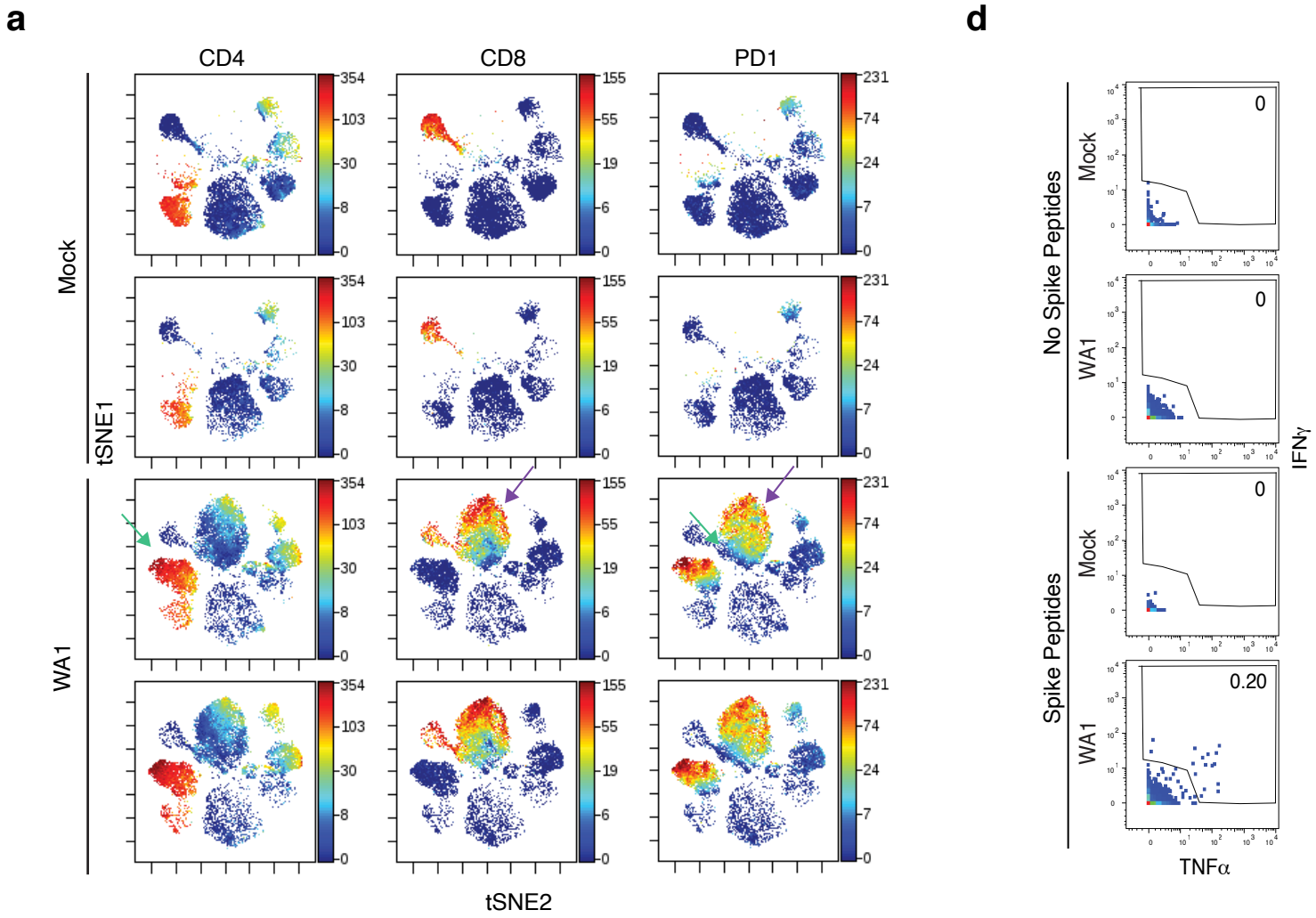

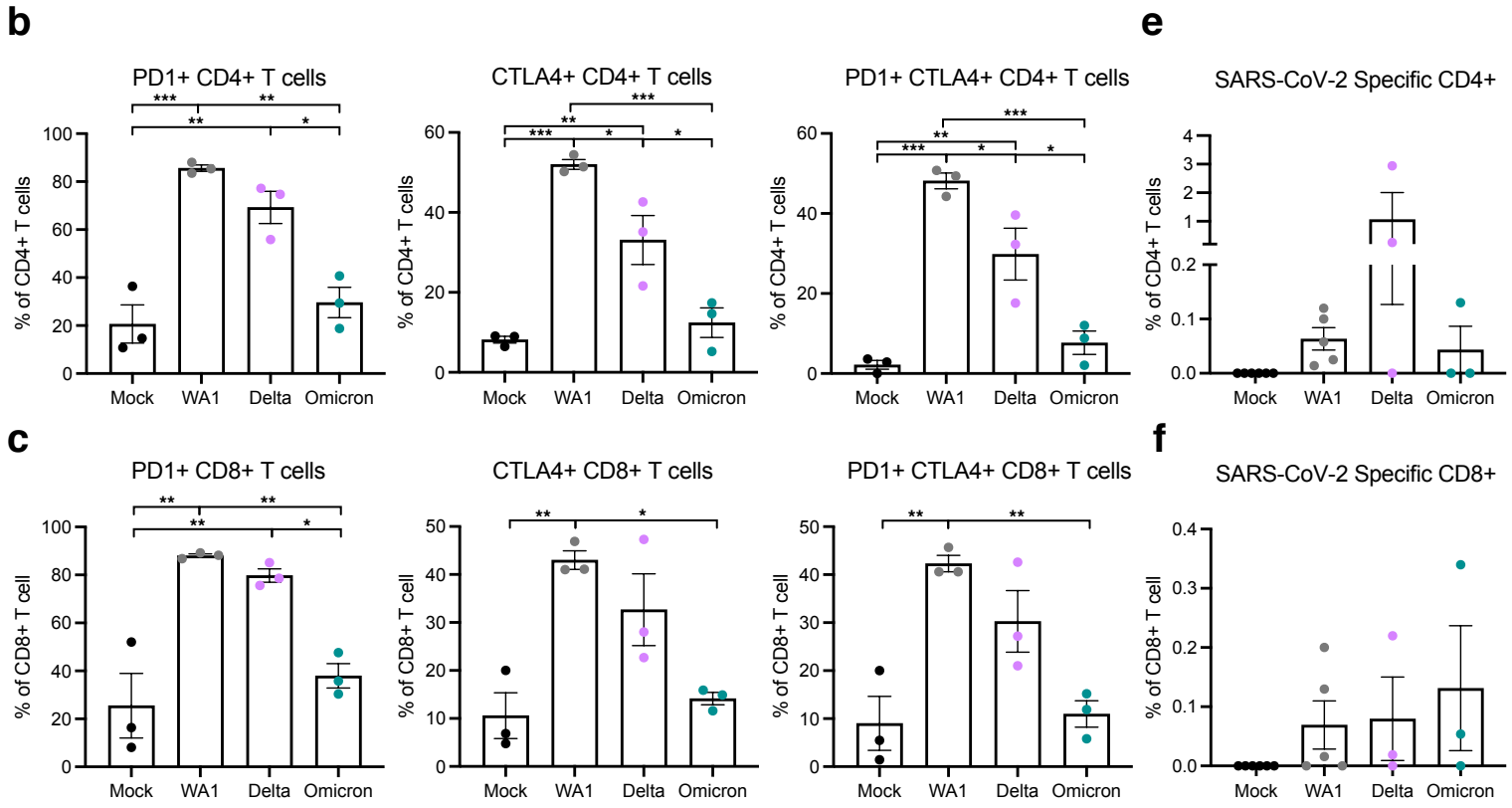

Fig. 4

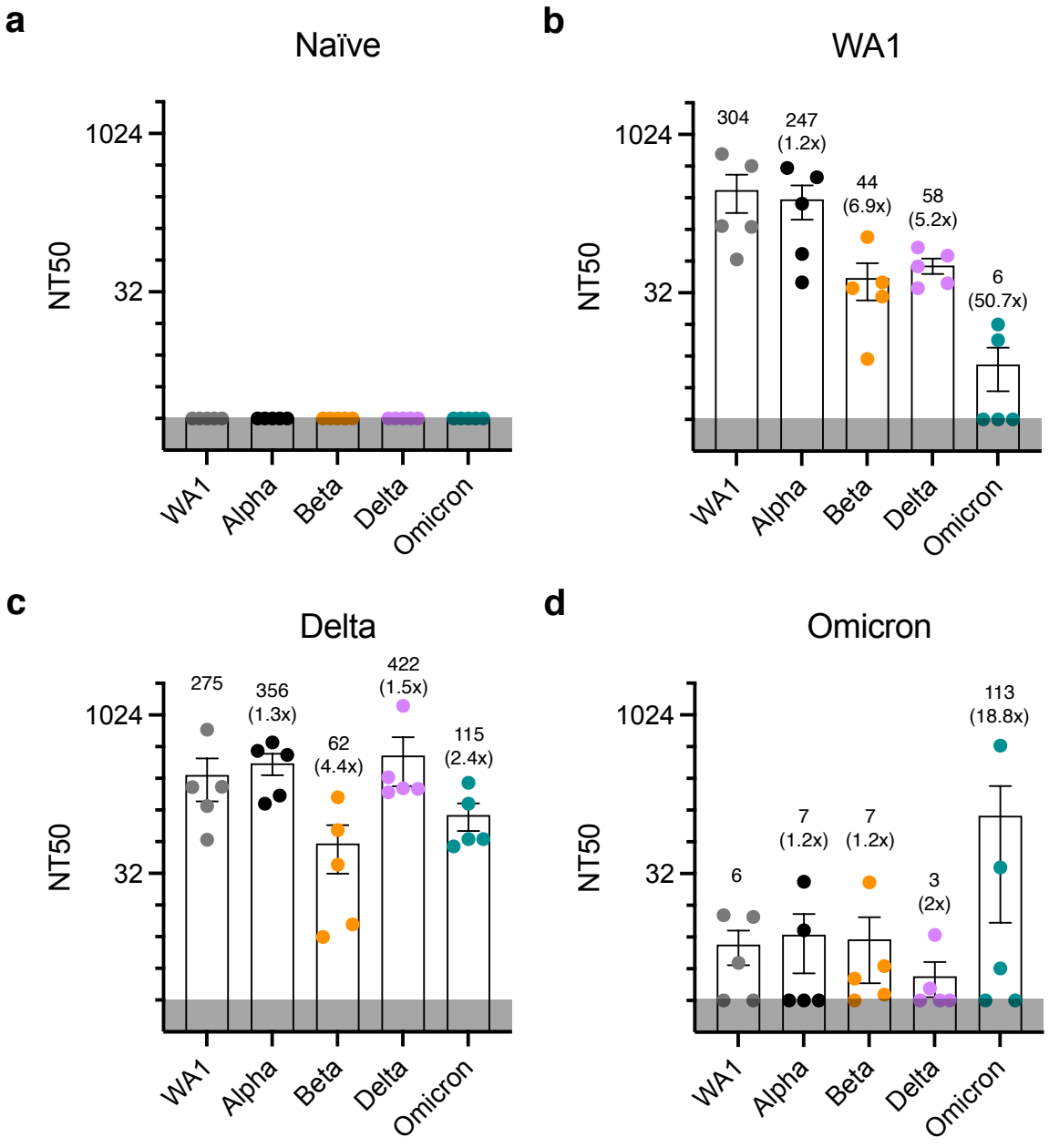

Fig. 5